European Radiology (2019) 29:6858–6866
https://doi.org/10.1007/s00330-019-06278-6

CHEST

Wide-volume versus helical acquisition in unenhanced chest CT: prospective intra-patient comparison of diagnostic accuracy and radiation dose in an ultra-low-dose setting

Elsa Meyer[1] · Aissam Labani[1] · Mickaël Schaeffer[1] · Mi-Young Jeung[1] · Claire Ludes[1] · Alain Meyer[2] · Catherine Roy[1] · Pierre Leyendecker[1] · Mickaël Ohana[1,3]

Received: 5 March 2019 / Revised: 15 April 2019 / Accepted: 17 May 2019 / Published online: 7 June 2019

Abstract

Objectives Diagnostic performance and potential radiation dose reduction of wide-area detector CT sequential acquisition ("wide-volume" acquisition (WV)) in unenhanced chest examination are unknown. This study aims to assess the image quality, the diagnostic performance, and the radiation dose reduction of WV mode compared with the classical helical acquisition for lung parenchyma analysis in an ultra-low-dose (ULD) protocol.

Methods After Institutional Review Board Approval and written informed consent, 64 patients (72% men; 67.6 ± 9.7 years old; BMI 26.1 ± 5.3 kg/m^2) referred for a clinically indicated unenhanced chest CT were prospectively included. All patients underwent, in addition to a standard helical acquisition (120 kV, automatic tube current modulation), two ULD acquisitions (135 kV, fixed tube current at 10 mA): one in helical mode and one in WV mode. Image noise, subjective image quality (5-level Likert scale), and diagnostic performance for the detection of 9 predetermined parenchymal abnormalities were assessed by two radiologists and compared using the chi-square or Fisher non-parametric tests.

Results Subjective image quality (4.2 ± 0.7 versus 4.2 ± 0.8, $p = 0.56$), image noise (41.7 ± 8 versus 40.9 ± 8.7, $p = 0.3$), and diagnostic performance were equivalent between ULD WV and ULD helical. Radiation dose was significantly lower for the ULD WV acquisition (mean dose-length product 14.1 ± 1.3 mGy cm versus 15.8 ± 1.3, $p < 0.0001$).

Conclusion An additional 11% dose reduction is achieved with the WV mode in ULD chest CT with fixed tube current, with equivalent image quality and diagnostic performance when compared with the helical acquisition.

Key Points

- *Image quality and diagnostic performance of ultra-low-dose unenhanced chest CT are identical between wide-volume mode and the reference helical acquisition.*
- *Wide-volume mode allows an additional radiation dose reduction of 11% (mean dose-length product 14.1 ± 1.3 mGy cm versus 15.8 ± 1.3, p < 0.0001).*

Keywords Multidetector computed tomography · Radiation dosage · Helical computed tomography · Lung

Abbreviations

ALARA	As Low As Reasonably Achievable
BMI	Body mass index
CT	Computed tomography
DLP	Dose-length product
ROI	Region of interest
SD	Standard deviation
ULD	Ultra-low dose
WV	Wide-volume

✉ Mickaël Ohana
mickael.ohana@gmail.com

[1] Radiology Department, Nouvel Hôpital Civil, 1 place de l'Hôpital, 67000 Strasbourg, France

[2] Physiology Department, Nouvel Hôpital Civil, 1 place de l'Hôpital, 67000 Strasbourg, France

[3] ICube Laboratory, 300 Boulevard Sébastien Brandt, 67400 Illkirch Graffenstaden, France

Introduction

Being the reference imaging method for the assessment of the lung parenchyma, chest computed tomography (CT) is a widely used examination, accounting for a high proportion of the collective dose delivered by this modality [1]. Following the ALARA (As Low As Reasonably Achievable) principle, radiologists should be aware of every option that could potentially reduce the radiation dose. Due to the high intrinsic contrast of the lung parenchyma and the low attenuation of the thoracic wall, unenhanced chest CT is a fitted candidate for a radical radiation dose reduction [2, 3].

Among the various technological improvements introduced to reduce the radiation dose delivered, wide-area detector CT could yield an interesting additional contribution. Based on a wide *z*-axis detection system (320 rows of 0.5 mm or 256 rows of 0.625 mm, both covering 16 cm), it allows the acquisition of a whole organ such as the heart, the brain, or the kidneys within a single rotation [4]. This "volume" acquisition can, compared with the standard helical one, reduce kinetic artifacts as well as radiation exposure [5]. The merging of sequential volume acquisitions combined with table motion between each gantry rotation enables the acquisition of a wider anatomical region such as the thorax or the abdomen and pelvis: this is called the "wide-volume" (WV) or "step and shoot" acquisition mode [6]. Its non-inferior image quality compared with the standard helical CT is demonstrated for the examination of the lumbar spine [7], the mediastinal arteries [8, 9], the small abdominal vessels [10], and the urinary excretory system [6], with a significant radiation dose reduction that can go up to 60% [8].

In chest imaging, the applicability of WV might be limited by breathing and motion resulting in stairstep artifacts. A preliminary study on 35 patients showed equivalence in image quality between the WV and the helical mode [11], however with a reported 14% CT dose index increase when using the WV mode. Thus, the potential utility of the WV mode regarding dose reduction in chest imaging is not well defined in the literature, and to date, no study has investigated its impact on the low-dose assessment of lung parenchyma.

The purpose of this study is, therefore, to assess the image quality, the diagnostic performance, and the radiation dose of the WV mode compared with the conventional helical acquisition for lung parenchyma analysis in an ultra-low-dose (ULD) setting.

Materials and methods

This prospective study was approved by our Institutional Review Board, and written informed consent was obtained from all participants.

Population

For 4 consecutive months, all in- and outpatients referred for a clinically indicated unenhanced chest CT outside of an emergency context were approached for participation. The only inclusion criterion was the minimum age of 40 years. The exclusion criteria were the inability to hold the breath for more than 3 s, the incapacity to raise the arms above the head, and the inability to give an informed consent.

Weight and height of each patient at the time of CT were recorded in order to calculate the body mass index (BMI).

CT examination and data reconstruction

All CT examinations were acquired on a second-generation 320-row scanner (Aquilion One Vision Edition, Canon Medical Systems).

Each patient underwent three successive unenhanced acquisitions: one standard-dose acquisition (120 kV with automated tube current modulation, called 120 kV helical) and two ultra-low-dose acquisitions (one acquired in helical mode, called ULD helical, and one acquired in WV mode, called ULD WV). The acquisition parameters are summarized in Table 1.

Patients were positioned supine, arms raised above the head, and had to realize three consecutive deep inspiration breathholds, one for each acquisition. The field of view was kept identical for all acquisitions. For the ULD WV acquisition, the number and length of sequential volumes required were automatically defined by the scanner.

Images were reconstructed at a 0.5-mm slice thickness using mediastinal and lung kernels, with iterative reconstruction (Adaptive Iterative Dose Reduction using 3 Dimensional AIDR-3D, Canon Medical Systems) set at a standard setting. For the ULD WV acquisition, the VolumeXact+® algorithm was used in order to overcome cone-beam artifacts, and a registered merging of the volumes (aka "stitching") was automatically performed.

Quantitative and qualitative image analyses

Image analysis was done exclusively on the lung parenchyma reconstructions. Three datasets (120 kV helical, ULD helical, and ULD WV) were available for each patient, and all were anonymized and randomized before analysis.

Quantitative image analysis

Image noise was defined as the standard deviation (SD) in Hounsfield units of the air attenuation measured in the tracheal lumen. An elliptical region of interest (ROI) of at least 10 mm^2 was drawn within the tracheal lumen 1 cm over the carina, on the lung parenchyma reconstruction, by the same investigator

Table 1 Acquisition parameters

	ULD WV	ULD Helical	120 kV helical
Tube voltage (kV)	135	135	120
Tube current (mA)	10 (fixed)	10 (fixed)	80–700 (automatic modulation)
Tube load (mAs)	3	3	20–200
Pitch	–	0.813	0.813
Rotation time (s)	0.275	0.275	0.275
Collimation	320 × 0.5 or 280 × 0.5 or 256 × 0.5 or 240 × 0.5	0.5 × 80	0.5 × 80
Slice thickness (mm)	0.5	0.5	0.5
Parenchymal reconstruction	0.5 mm every 0.3 mm	0.5 mm every 0.3 mm	0.5 mm every 0.3 mm
Reconstruction algorithm	AIDR-3D VolumeXact +®	AIDR-3D	AIDR-3D

(EM, with 4 years of experience in CT). Measurements were repeated three times for each acquisition, keeping reproducible ROI size and location; the mean SD value was used as the image noise quantification.

Qualitative image analysis

CT images were independently assessed by two readers: a senior radiologist specialized in chest imaging (MO, with 8 years of experience in CT) and a junior radiologist (EM, with 4 years of experience). Reading sessions were conducted on a dedicated workstation (Vitrea Version 6.4, Canon Medical Systems). The default window setting (width 1500 HU and level 700 HU) could be adapted by each reader. Multiplanar reconstructions, as well as 5-mm-thickness maximum intensity projection reconstructions, were systematically used.

Overall image quality analysis Both readers were asked to independently evaluate the subjective image quality of all examinations, using a 5-level Likert scale (1 = non-diagnostic image quality to 5 = excellent image quality). The overall image quality evaluation was based on the spatial resolution, the neatness of the anatomical structures, and the presence and the severity of artifacts, especially misalignment on coronal and sagittal multiplanar reconstructions. Scores of 1 and 2 were judged to be of non-diagnostic image quality, while scores from 3 to 5 were considered to be of diagnostic quality.

Diagnostic performance For every acquisition, both readers were asked to identify the presence or absence of a list of predefined lung parenchymal abnormalities. These items were based on the Fleischner Society glossary of terms [12] and consisted of solid lung nodule greater than 5 mm, ground-glass nodule, mass (greater than 3 cm), ground-glass opacity, alveolar consolidation, emphysema, interstitial septal thickening, bronchiectasis, and fibrosis. The number of solid nodules greater than 5 mm and the number of ground glass nodule were also recorded.

The gold standard was defined by the reading of the 120-kV helical acquisition, with discrepancies between readers resolved by consensus. For each reader, the analysis of the ULD helical and the ULD WV acquisitions was compared to this gold standard, to calculate a sensitivity, specificity, positive predictive value, and negative predictive value.

Radiation dose evaluation

The dose-length product (DLP) in milligray centimeter (mGy cm) was recorded for each of the three acquisitions. The estimated effective dose (ED) in millisievert (mSv) was calculated with the formula $ED = DLP \times k$, with k being the specific chest conversion factor ($k = 0.014$ mSv/mGy cm) [13].

Body mass index

Influence of BMI on noise and image quality

Potential correlations between the BMI and the noise and the BMI and the subjective image quality were sought using a Spearman correlation coefficient.

Influence of BMI on diagnostic performance

The diagnostic performances of the ULD helical and ULD WV acquisitions for the 9 predefined parenchymal

abnormalities were compared according to BMI classes, to detect a potential negative influence of the latter.

Statistical analysis

All recorded variables were compared between 120-kV helical, ULD helical, and ULD WV groups using the chi-square tests or Fisher non-parametric test for proportions, depending on the theoretical effectiveness. To check for the Gaussian distribution, the Shapiro-Wilk test for normality was used. The Student *t* test or Mann-Whitney U test was used to compare numerical data. Results are presented in mean ± standard deviation.

Non-inferiority was evaluated by calculating the confidence interval of the difference between the two groups. The lower bound of the one-sided interval was then compared to 5% to conclude.

Diagnostic performance of all measures was evaluated by sensibility, specificity, and positive and negative predictive values.

Concordance between readers was measured by Cohen's kappa interval.

A total of 10,000 bootstrap replications were used to estimate the associated confidence interval and then to test the coefficient to 0. All statistical tests were two-tailed. A p value < 0.05 was considered statistically significant. In order to avoid the inflation of the risk alpha while comparing the 4 groups, pairwise tests were done with a correction of the p value according to the Holms method.

All analyses were performed using R software under its version 3.0 (R Core Team (2014). R: A language and environment for statistical computing).

Results

Population

Seventy-one patients were approached and 7 declined participation in the study. Sixty-four patients (mean age 67.6 ± 9.7 years, range 42–88) were ultimately included: 46 men (mean age 66.8 ± 9.0 years) and 18 women (mean age 69.7 ± 10.9 years).

Clinical indications for the chest CT included follow-up of pulmonary nodule (22/64 patients, 35%), suspicion of lung infections or follow-up of treated lung infections (10 patients, 16%), follow-up of chronic obstructive pulmonary disease (7 patients, 10%), oncologic follow-up (6 patients, 9%), follow-up of interstitial pneumonia (6 patients, 9%), and other indications (13 patients, 21%).

The mean BMI was 26.1 ± 5.3 kg/m^2 (min 14.4–max 40.6) with 33 patients (52%) having a BMI ≤ 25, 18 patients (28%) a BMI between 25 and 30, and 13 patients (20%) a BMI ≥ 30.

Quantitative and qualitative image analyses

Quantitative image analysis

Image noise was identical on the ULD helical (40.92 ± 8.7) and the ULD WV (41.69 ± 8) acquisitions ($p = 0.3$), compared with 29.86 ± 5.9 for the 120 kV helical.

Qualitative image analysis

Overall image quality analysis There were no significant differences in subjective image quality rating between both ULD acquisitions whether by readers (reader 1 4.2 ± 0.7 for the ULD WV and 4.2 ± 0.8 for the ULD helical, $p = 0.55$; reader 2 4.4 ± 0.7 and 4.4 ± 0.7, respectively, $p = 1$) (Table 2) or when pooling the scores of both readers (4.2 ± 0.7 for the ULD WV and 4.2 ± 0.8 for the ULD helical, $p = 0.56$) (Fig. 1). The overall image quality was considered diagnostic in 99.2% of cases for the ULD WV as well as for the ULD helical. The inter-reader agreement was low, with a Cohen's kappa at 0.30 (0.17–0.43).

Diagnostic performance Diagnostic performance of the ULD WV regarding the 9 lung parenchymal abnormalities was not inferior to the ULD helical, with a threshold of 5% ($p > 0.005$).

Detailed sensitivity and specificity for each reader are given in Table 3. On average for both readers, the sensitivity of the ULD WV was 100% for masses, 96.5% for alveolar consolidation, 95.5% for solid nodules (Fig. 1), 93% for ground-glass opacity, 80.5% for emphysema (Fig. 2), 66% for bronchiectasis (Fig. 3), 42.5% for fibrosis, and 37.5% for interstitial septal thickening.

The inter-reader agreement was:

- Substantial (Cohen's kappa, 0.61–0.80) for solid nodule greater than 5 mm, mass, ground-glass opacity, alveolar consolidation, and emphysema.

Table 2 Distribution of ULD IQ scores assigned by both readers. Results given as numbers (percentages)

Notes	ULD helical		ULD WV	
	L1	L2	L1	L2
1	0 (0%)	0 (0%)	0 (0%)	0 (0%)
2	0 (0%)	1 (1.6%)	0 (0%)	1 (1.6%)
3	16 (25%)	6 (9.4%)	12 (18.8%)	6 (9.4%)
4	21 (31.8%)	20 (31.2%)	26 (40.6%)	20 (31.2%)
5	27 (42.2%)	37 (57.8%)	26 (40.8%)	37 (57.8%)
Average ± SD	4.17 ± 0.80	4.45 ± 0.73	4.21 ± 0.74	4.45 ± 0.73

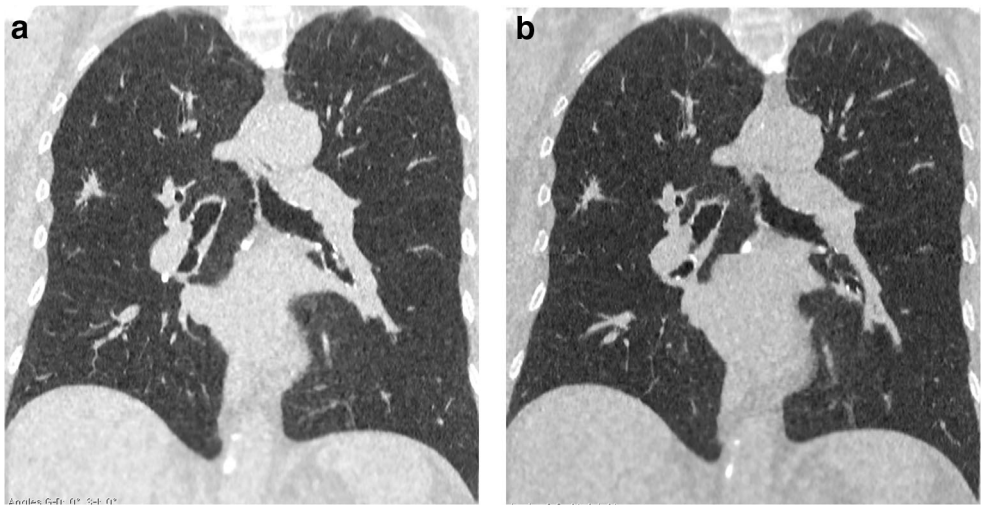

Fig. 1 Sagittal reconstruction of an ULD chest CT acquired in helical mode (**a**) and WV mode (**b**) in a 87-year-old woman with a BMI of 25 kg/m^2. This example shows the equivalence of the ULD helical (a, DLP 14.2 mGy cm) and ULD WV (b, DLP 13.2 mGy cm) for the diagnosis of solid nodule

Table 3 Detailed sensitivity and specificity of ULD helical and ULD WV for each reader

	ULD helical		ULD WV	
	Sensitivity	Specificity	Sensitivity	Specificity
Nodule ($n = 32$)				
Reader 1	84% (27/32)	97% (30/31)	94% (30/32)	91% (29/32)
Reader 2	91%0 (29/32)	100% (32/32)	91% (29/32)	100% (32/32)
Ground-glass nodule ($n = 3$)				
Reader 1	33% (1/3)	97% (59/61)	0% (0/3)	97% (59/61)
Reader 2	100% (3/3)	97% (59/61)	100% (3/3)	97% (59/61)
Mass ($n = 1$)				
Reader 1	100% (1/1)	100% (63/63)	100% (1/1)	100% (63/63)
Reader 2	100% (1/1)	100% (63/63)	100% (1/1)	100% (63/63)
Ground-glass opacity ($n = 14$)				
Reader 1	71% (10/14)	94% (47/50)	93% (13/14)	94% (47/50)
Reader 2	93% (13/14)	100% (50/50)	93% (13/14)	100% (50/50)
Alveolar consolidation ($n = 14$)				
Reader 1	93% (13/14)	92% (46/50)	93% (13/14)	96% (48/50)
Reader 2	100% (14/14)	100% (50/50)	100% (14/14)	100% (50/50)
Emphysema ($n = 28$)				
Reader 1	79% (22/28)	100% (36/36)	86% (24/28)	94% (34/36)
Reader 2	75% (21/28)	92% (33/36)	75% (21/28)	92% (33/36)
Interstitial septal thickening ($n = 4$)				
Reader 1	50% (2/4)	98% (59/60)	25% (1/4)	100% (60/60)
Reader 2	50% (2/4)	100% (60/60)	50% (2/4)	100% (60/60)
Bronchiectasis ($n = 16$)				
Reader 1	56% (9/16)	92% (44/48)	44% (7/16)	98% (47/48)
Reader 2	88% (14/16)	96% (46/48)	88% (14/16)	96% (46/48)
Fibrosis ($n = 7$)				
Reader 1	29% (2/7)	100% (57/57)	14% (1/7)	100% (57/57)
Reader 2	71% (5/7)	100% (57/57)	71% (5/7)	100% (57/57)

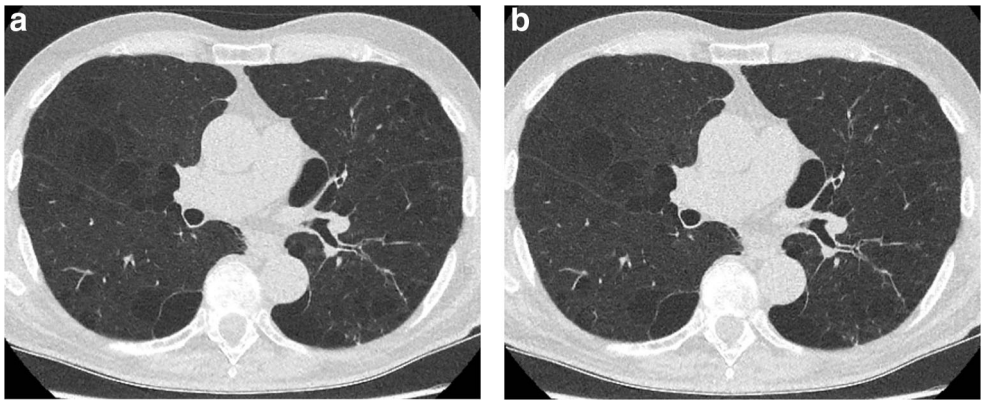

Fig. 2 Axial ULD chest CT acquired in helical mode (**a**) and WV mode (**b**) in a 88-year-old man with a BMI of 23 kg/m^2. This example shows the equivalence of the ULD helical (a, DLP 17.1 mGy cm) an the ULD WV (b, DLP 13.2 mGy cm) for the diagnosis of emphysema

- Moderate (Cohen's kappa, 0.41–0.60) for interstitial septal thickening, bronchiectasis, and fibrosis.
- None to slight (Cohen's kappa, 0–0.20) for ground-glass nodule.

Radiation dose evaluation

The mean radiation dose was 14.1 ± 1.3 mGy cm (min 10.8–max 16.8, corresponding to 0.20 ± 0.02 mSv) for the ULD WV and 15.8 ± 1.3 mGy cm (min 12.5–max 18.4, 0.22 ± 0.02 mSv) for the ULD helical. The average radiation dose was therefore significantly lower for the ULD VW, with a mean dose reduction of 11% ($p < 0.0001$).

As a comparison, the mean radiation dose of the 120 kV helical was 247.7 ± 119 mGy cm (min 84.2–max 793, corresponding to 3.47 ± 1.7 mSv).

Influence of the BMI

Influence of the BMI on noise and image quality

The BMI negatively influences the image noise and the subjective image quality in the ULD helical as well as in the ULD WV (Table 4).

Influence of BMI on diagnostic performance

The BMI significantly negatively influences ($p < 0.05$) the sensitivity and specificity of emphysema and fibrosis diagnosis in both ULD helical and ULD WV. For the other parenchymal abnormalities, the BMI has no significant influence on the specificity or sensitivity whatever the technique of acquisition. This parameter could not be studied for the masses due to a too low number of cases.

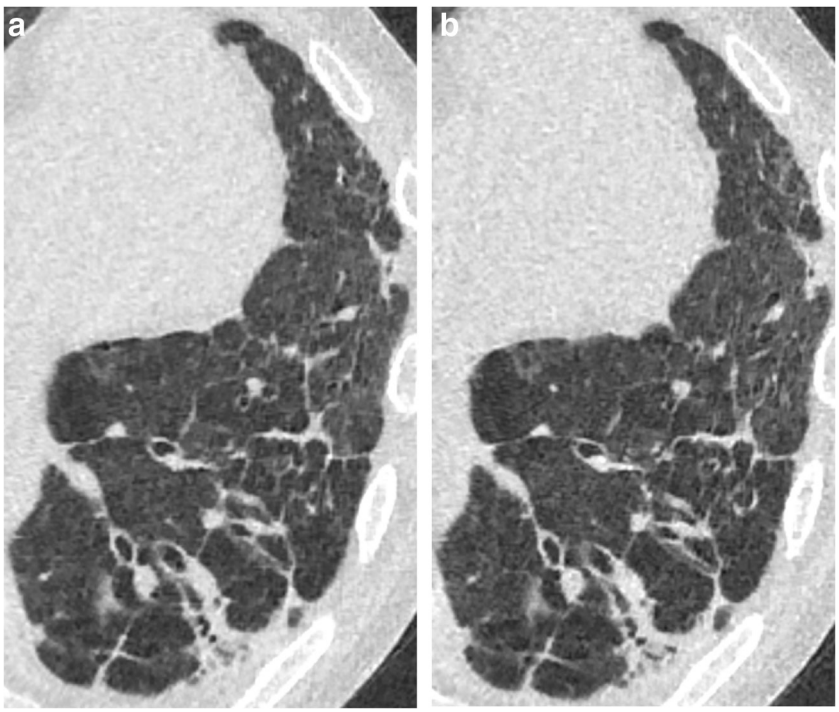

Fig. 3 Axial ULD chest CT acquired in helical mode (**a**) and WV mode (**b**) in a 53-year-old man with a BMI of 23 kg/m^2. This example shows the equivalence of the ULD helical (a, DLP 16.5 mGy cm) and the ULD WV (b, DLP 16.2 mGy cm) for the diagnosis of bronchiectasis

Table 4 Correlation of noise and subjective image quality with BMI

Correlation with BMI (Spearman correlation coefficient)	ULD helical	ULD WV	*p*
Noise	− 0.682	− 0.693	< 0.01
Image quality	− 0.478	− 0.409	< 0.01

Discussion

This study demonstrates that ULD chest CT acquired in WV mode using a wide-area detector scanner performs identically (the same objective and subjective image quality and the same diagnostic performance) to the reference helical acquisition, while achieving a significant additional radiation dose reduction of 11%, in an ultra-low-dose protocol with a fixed exposure. Lung parenchyma being sensitive to respiratory- and cardiac-induced motion artifacts, one could fear that stairstep artifacts would appear between two contiguous volumes when using a WV acquisition [8]. In our work, ULD WV acquisitions were subjectively and quantitatively equivalent to the ULD helical acquisitions, without any deleterious artifact at the junctions, confirming the efficiency of the image stitching algorithm (Fig. 4). This is on par with what was found by Honda et al on 35 cases [11].

In our work, the diagnostic performance of the ULD WV and the ULD helical was equivalent (Table 3) and in accordance with prior published ULD chest CT studies: sensitivity of 70–100% for the detection of solid lung nodule [14–18], sensitivity of 63–65% for alveolar consolidation [16, 19] and ground-glass opacities [16], sensitivity of 65–69% for ground-glass nodules [15–17], and a lower sensitivity of 47–75% for emphysema [15, 20] and interstitial lesions [21, 22]. The relatively important inter-reader difference for ground-glass nodules and interstitial lesions might be explained by the low number of these lesions and by the difference in experience between readers.

The radiation dose reduction achieved in our study was relatively low at 11%. This is partly explained by the fact that we have voluntarily worked with an ultra-low-dose protocol. This was motivated by the will of doing an intra-patient comparison, since it would have been difficult to ethically justify the repetition of a full-dose acquisition in WV mode. This choice also made it possible to neutralize other potential confounding factors such as the automated tube current modulation, which is not used in our ULD acquisition protocol [23]. Finally, this choice was also logical to explore an additional dose-saving option in the ULD space.

In a "standard-dose" chest CT protocol using automated tube current modulation, the radiation dose reduction provided by the WV technique could be greater, as observed for other organs with a decrease of 35% for the lumbar spine CT [24] and 44% for CT urography [6]. However, data concerning WV chest CT in the literature are contradictory. In a chest CT angiography study, the dose reduction in WV mode was approximately 60% in a triple rule-out protocol for a simultaneous study of the aorta, the pulmonary arteries, and the coronary arteries [8]. On the contrary, another study on a similar chest pain CTA protocol did not find any difference in radiation dose between WV and helical [25]. Regarding unenhanced chest CT and lung parenchyma exploration, studies are scarce and their results also are conflicting. In a work on a pediatric phantom model, Johnston et al demonstrated a dose reduction ranging from 27 to 46% but compared a helical mode on a 64-row scanner [26]. Both acquisitions were made with automated tube current modulation, but active

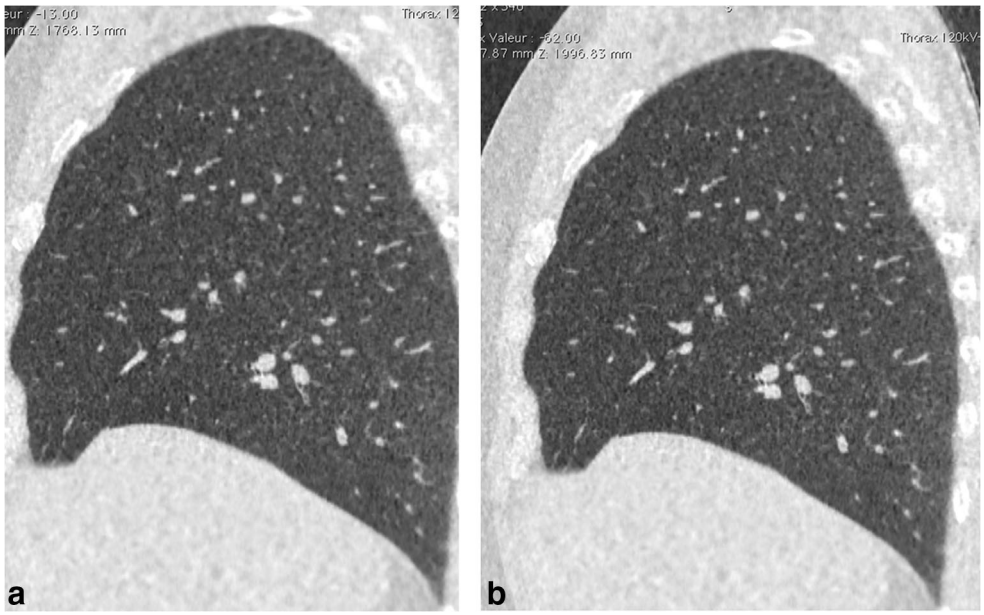

Fig. 4 Sagittal ULD chest CT acquired in helical mode (**a**) and wide-volume mode (**b**) in a 59-year-old man with a BMI of 22.5 kg/m^2. This example shows that "stairstep artifacts" can hardly be discerned on ULD WV, thanks to the automatic stitching algorithm. DLP, 16.5 mGy cm for ULD helical and 15.2 mGy cm in ULD WV

collimation was used only for WV, which is a potential bias since it enables a dose reduction of up to 30% [27]. Yamashiro et al demonstrated a similar radiation dose between WV and helical in a protocol without automated tube current modulation and iterative reconstruction techniques [28]. Lastly, Honda et al showed an increase in the CT dose index of 14% in WV versus helical using comparable acquisition parameters [11], however with an earlier version of the WV software; the final DLP of both acquisitions was not reported. The strength of our study is to have an intra-patient comparison and strictly identical acquisition parameters between ULD WV and ULD helical, which allows us to assert that the observed dosimetric difference is strictly related to the use of a WV acquisition.

The dose reduction achieved by using the WV mode is explained by the phenomena of overranging, overbeaming, and overlapping [6]. Overranging corresponds to the additional rotation at both ends of the acquisition in a helical mode and does not exist when using sequential WV acquisition [29]. Overbeaming refers to the excess in radiation at each rotation which is not useful for image reconstruction. Its relative significance decreases proportionally with the width of the detectors and is thus lower with a wider detection system that is used in WV mode [30]. Overlapping refers to the overlap of volumes; it is reduced in WV because it occurs only at the junction between 2 volumes, whereas in helical mode, it occurs at each helical rotation when the pitch is less than 1 [6].

This work has limitations.

The first one is the relatively small size of the sample with 64 patients, which is nevertheless sufficient to demonstrate the diagnostic and qualitative non-inferiority of the ULD WV compared with the ULD helical, with a threshold of 5%.

The second limitation is induced by the choice of a ULD mode with a fixed tube current without automatic modulation [23]. In helical mode with a conventional protocol, an automatic tube current modulation based on the analysis of the topogram takes place throughout the acquisition [27]. In WV mode, the acquisition of a volume can only be done with a fixed tube current, and an automatic tube current modulation would occur only between two volumes, inducing an increase of the offset artifact with a difference in density between volumes [31]. Thus, our results are valid for the ULD mode with a fixed tube current, but cannot be completely extrapolated to a standard mode where automated tube current modulation would be used [32].

To conclude, this work demonstrates that chest CT acquired in wide-volume mode have identical image quality and diagnostic performance for the exploration of lung parenchyma compared with the classical helical acquisition, with the advantage of a significant radiation dose of 11%, in an ultra-low-dose protocol. Further studies should be carried out to extrapolate these results to a "standard-dose" chest CT scan, where the dose reduction achieved by the addition of a WV technique could potentially be greater.

Acknowledgments The authors would like to thank Mr. Karim Haioun for his help in implementing the technical aspects of this study.

Funding The authors state that this work has not received any funding.

Compliance with ethical standards

Guarantor The scientific guarantor of this publication is Dr. Mickaël Ohana.

Conflict of interest The authors of this manuscript declare no relationships with any companies whose products or services may be related to the subject matter of the article.

Statistics and biometry One of the authors has significant statistical expertise: Dr. Mickaël Schaeffer is a biostatistician.

Informed consent Written informed consent was obtained from all subjects (patients) in this study.

Ethical approval Institutional Review Board approval was obtained.

Methodology
- Prospective
- Case-control study
- Performed at one institution

References

1. Smith-Bindman R, Wang Y, Chu P et al (2019) International variation in radiation dose for computed tomography examinations: prospective cohort study. BMJ 364:k4931
2. Ohana M, Ludes C, Schaal M et al (2017) What future for chest x-ray against ultra-low-dose computed tomography? Rev Pneumol Clin 73:3–12
3. Ludes C, Schaal M, Labani A, Jeung MY, Roy C, Ohana M (2016) Ultra-low dose chest CT: the end of chest radiograph. Presse Med 45:291–301
4. Patel N, Li D, Nakanishi R et al (2019) Comparison of whole heart computed tomography scanners for image quality lower radiation dosing in coronary computed tomography angiography: the CONVERGE registry. Acad Radiol. https://doi.org/10.1016/j.acra.2019.01.002
5. Mata-Mbemba D, Labani A, El Ghannudi S et al (2018) 320-row CT transcatheter aortic valve replacement planning with a single reduced contrast media bolus injection. PLoS One 13:e0204145
6. Roy C, Quin R, Labani A, Leyendecker P, Mertz L, Ohana M (2018) Wide volume versus helical acquisition using 320-detector row computed tomography for computed tomography urography in adults. Diagn Interv Imaging 99:653–662
7. Gervaise A, Teixeira P, Villani N, Lecocq S, Louis M, Blum A (2013) CT dose optimisation and reduction in osteoarticular disease. Diagn Interv Imaging 94:371–388
8. Kang EJ, Lee KN, Kim DW et al (2012) Triple rule-out acute chest pain evaluation using a 320-row-detector volume CT: a comparison of the wide-volume and helical modes. Int J Cardiovasc Imaging 28(Suppl 1):7–13

9. Durmus T, Rogalla P, Lembcke A, Muhler MR, Hamm B, Hein PA (2011) Low-dose triple-rule-out using 320-row-detector volume MDCT-less contrast medium and lower radiation exposure. Eur Radiol 21:1416–1423
10. Kitajima K, Maeda T, Ohno Y et al (2011) Capability of abdominal 320-detector row CT for small vasculature assessment compared with that of 64-detector row CT. Eur J Radiol 80:219–223
11. Honda O, Takenaka D, Matsuki M et al (2012) Image quality of 320-detector row wide-volume computed tomography with diffuse lung diseases: comparison with 64-detector row helical CT. J Comput Assist Tomogr 36:505–511
12. Hansell DM, Bankier AA, MacMahon H, McLoud TC, Muller NL, Remy J (2008) Fleischner society: glossary of terms for thoracic imaging. Radiology 246:697–722
13. Huda W, Ogden KM, Khorasani MR (2008) Converting dose-length product to effective dose at CT. Radiology 248:995–1003
14. Yoon HJ, Chung MJ, Hwang HS, Moon JW, Lee KS (2015) Adaptive statistical iterative reconstruction-applied ultra-low-dose CT with radiography-comparable radiation dose: usefulness for lung nodule detection. Korean J Radiol 16:1132–1141
15. Neroladaki A, Botsikas D, Boudabbous S, Becker CD, Montet X (2013) Computed tomography of the chest with model-based iterative reconstruction using a radiation exposure similar to chest X-ray examination: preliminary observations. Eur Radiol 23:360–366
16. Lee SW, Kim Y, Shim SS et al (2014) Image quality assessment of ultra low-dose chest CT using sinogram-affirmed iterative reconstruction. Eur Radiol 24:817–826
17. Nagatani Y, Takahashi M, Murata K et al (2015) Lung nodule detection performance in five observers on computed tomography (CT) with adaptive iterative dose reduction using three-dimensional processing (AIDR 3D) in a Japanese multicenter study: comparison between ultra-low-dose CT and low-dose CT by receiver-operating characteristic analysis. Eur J Radiol 84:1401–1412
18. Messerli M, Kluckert T, Knitel M et al (2017) Ultralow dose CT for pulmonary nodule detection with chest x-ray equivalent dose - a prospective intra-individual comparative study. Eur Radiol 27:3290–3299
19. Kim HJ, Park SY, Lee HY, Lee KS, Shin KE, Moon JW (2014) Ultra-low-dose chest CT in patients with neutropenic fever and hematologic malignancy: image quality and its diagnostic performance. Cancer Res Treat 46:393–402
20. Wang R, Sui X, Schoepf UJ et al (2015) Ultralow-radiation-dose chest CT: accuracy for lung densitometry and emphysema detection. AJR Am J Roentgenol 204:743–749
21. Tekath M, Dutheil F, Bellini R et al (2014) Comparison of the ultra-low-dose Veo algorithm with the gold standard filtered back projection for detecting pulmonary asbestos-related conditions: a clinical observational study. BMJ Open 4:e004980
22. Schaal M, Severac F, Labani A, Jeung MY, Roy C, Ohana M (2016) Diagnostic performance of ultra-low-dose computed tomography for detecting Asbestos-related pleuropulmonary diseases: prospective study in a screening setting. PLoS One 11:e0168979
23. Ludes C, Labani A, Severac F et al (2019) Ultra-low-dose unenhanced chest CT: prospective comparison of high kV/low mA versus low kV/high mA protocols. Diagn Interv Imaging 100:85–93
24. Gervaise A, Louis M, Batch T et al (2010) Dose reduction at CT of the lumbar spine using a 320-detector row scanner: initial results. J Radiol 91:779–785
25. Hein PA, Romano VC, Lembcke A, May J, Rogalla P (2009) Initial experience with a chest pain protocol using 320-slice volume MDCT. Eur Radiol 19:1148–1155
26. Johnston JH, Podberesky DJ, Yoshizumi TT et al (2013) Comparison of radiation dose estimates, image noise, and scan duration in pediatric body imaging for volumetric and helical modes on 320-detector CT and helical mode on 64-detector CT. Pediatr Radiol 43:1117–1127
27. Kalra MK, Maher MM, Toth TL, Kamath RS, Halpern EF, Saini S (2004) Comparison of Z-axis automatic tube current modulation technique with fixed tube current CT scanning of abdomen and pelvis. Radiology 232:347–353
28. Yamashiro T, Miyara T, Takahashi M et al (2012) Lung image quality with 320-row wide-volume CT scans: the effect of prospective ECG-gating and comparisons with 64-row helical CT scans. Acad Radiol 19:380–388
29. Schilham A, van der Molen AJ, Prokop M, de Jong HW (2010) Overranging at multisection CT: an underestimated source of excess radiation exposure. Radiographics 30:1057–1067
30. Sorantin E, Riccabona M, Stucklschweiger G, Guss H, Fotter R (2013) Experience with volumetric (320 rows) pediatric CT. Eur J Radiol 82:1091–1097
31. Liao YL, Lai NK, Tyan YS, Chuang KS, Tsai HY (2013) Automatic tube current modulation for volume scan in a 320-detector row CT scanner. Radiat Meas 328–332. https://doi.org/10.1016/j.radmeas.2013.04.012
32. Svahn TM, Sjoberg T, Ast JC (2018) Dose estimation of ultra-low-dose chest CT to different sized adult patients. Eur Radiol. https://doi.org/10.1007/s00330-018-5849-5